Progress In Electromagnetics Research C, Vol. 68, 107–117, 2016

A Novel High-Gain Directional Lens Antenna for Terahertz Band

Wu Pan, Wei Zeng*, Xuan Yu, and Jun Zhang

Abstract—A novel high-gain directional lens antenna is numerically designed and experimentally tested in terahertz atmospheric transmission I window. The lens antenna consists of two components: a diagonal horn is adopted as the primary feed antenna, and a multilayer stacked lens consisting of the concentric hatch-crosses is used to focus the electromagnetic waves. The far-field characteristics of the horn antenna and the lens antenna are both studied. Furthermore, the effects of the number of periods of the lens and the focus diameter ratio on radiation characteristics are studied by using variable-controlling approach. The experimental results show that both the diagonal horn antenna and the lens antenna have axisymmetric radiation patterns. The gain of the horn antenna ranges from 23.8 dB to 24.9 dB, and the 3 dB main lobe beamwidth varies from 10.8° to 12.4°. The gain of the lens antenna is higher than 26.4 dB, and the 3 dB main lobe beamwidth is lower than 4.8° across the operation bandwidth. The good focusing characteristics and great directionality indicate that the designed lens antenna is qualified for applications in THz wireless communication systems.

1. INTRODUCTION

Terahertz (THz) frequency range is roughly defined as 0.1–10 THz, which lies in the transition region from the microwaves to the infrared [1]. Antenna, which plays a momentous role in wireless communication systems, transforms converting guided waves into radiating waves travelling in free space, or vice versa [2]. Since the atmospheric path loss is significant [3, 4], the THz wireless communication system is usually a point-to-point system [5, 6]. Therefore, the art of THz antenna design is to ensure that the antenna is able to radiate as much power from the transmitter into a particular direction.

To improve the gain and directionality of the antenna, various types of lenses derived from optics fields, such as cylindrical lens [7], hemi-elliptical lens [8], Gaussian optic lens [9] and Fresnel zone plate lens [10], have been studied and used to focus electromagnetic waves. In 2011, Llombart et al. [11] proposed an extended hemispherical lens antenna fed by a leaky waveguide feed at frequencies from 510 to 600 GHz, where a couple of TE/TM leaky wave modes are excited in a resonant cavity formed by a waveguide opening ground plane and a silicon lens. The maximum directivity of roughly 27 dB has been achieved for the lens diameter $R = 6$ mm. In 2014, Singh et al. [12] have presented a phase correcting-Fresnel zone plate antenna for band ranging from 26 GHz to 34 GHz. The surface of the designed Fresnel lens antenna is composed of unit cells of small rectangular lattices which are converted into continuous large rectangular cells. The gain of 22.1 dB and 3 dB main lobe beamwidth of 22.1° are obtained at 30 GHz. Compared with conventional plano-hyperbolic lens antenna, the Fresnel zone plate lens antenna has an extremely small thickness. However, few investigations on lens antenna in THz band have been presented. Nevertheless, further enhancement in gain and directionality is still required for THz wireless communication systems.

In order to improve the focusing gain and directionality further, a novel lens antenna is presented in the article. A diagonal horn is numerically designed firstly which is adopted as the primary feed antenna.

Received 30 May 2016, Accepted 2 October 2016, Scheduled 13 October 2016
* Corresponding author: Wei Zeng (vlad_zehn@163.com).
The authors are with the College of Photoelectric Engineering, Chongqing University of Posts and Telecommunications, Chongqing 400065, China.

Then the multilayer stacked lens consisting of concentric hatch-crosses to focus electromagnetic waves is studied. Effects of the number of periods of the lens and the focus diameter ratio on the antenna radiation characteristics are studied by using variable-controlling approach. The experimental results indicate that the designed lens antenna has a high gain over 26.4 dB and a low 3 dB main lobe beamwidth less than 4.8° throughout the whole operation bandwidth. In other words, the proposed lens antenna has good focusing properties and great directionality.

2. THEORETICAL ANALYSIS AND GENERAL DESIGN

According to the absorption model of THz waves in atmosphere, there is a cursory 60 GHz frequency band suited for THz wireless communication around 350 GHz, which is called THz atmospheric transmission I window [13]. Therefore, the center operation frequency is 350 GHz, and the working band ranges from 320 GHz to 380 GHz in the article.

In the optical field, the Fresnel zone plate (FZP) lenses are commonly used to focus the light beams. The most typical FZP lens designs have annular Fresnel zones (rings). Based on the analysis of the focusing action and design rules of the typical FZP lens consisting of annular rings, the multilayer stacked lens consisting of the concentric hatch-crosses is proposed by applying the paraxial approximation and the phase compensation to the annular Fresnel zones to focus terahertz waves. As shown in Figure 1(a), the concentric hatch-crosses are stacked tightly one by one. A plane wave travelling along the axis Z which is represented by paraxial rays, illuminates the lens from the smaller ring side. After refraction through the concentric hatch-crosses, the incident plane wave is converted into a spherical one, and the parallel rays are focused at the primary focal point P. The focusing field produced by the lens on the axis Z is analyzed by using Fresnel-Kirchhoff diffraction theory. For simplicity, the flat annular ring in Figure 1(b) is analyzed firstly as follows.

The aperture unit dA' in Figure 1(b) produces a focusing field dE_n at any point P' on axis Z which is given by [14–16]

$$dE_n(r'_n) = \frac{j}{\lambda} E_0(Z'_n) e^{-j\Delta\Phi_n} H(\psi) \frac{e^{-j\beta r'_n}}{r'_n} dA \tag{1}$$

where $H(\psi) = (1+\cos\psi)/2$ is the Huygens source factor; $r'_n = \sqrt{(Z'_n - Z_n)^2 + R^2}$ is the distance between points Q and P'; $E_0(Z'_n) = E_0 e^{-j\beta Z'_n}$ represents the plane wave at point P' without the lens; $\Delta\Phi_n = \beta[Z_n + w_n(\sqrt{\varepsilon} - 1)]$ is a phase shift owing to the ring; $\beta = 2\pi/\lambda$ is the free-space phase number.

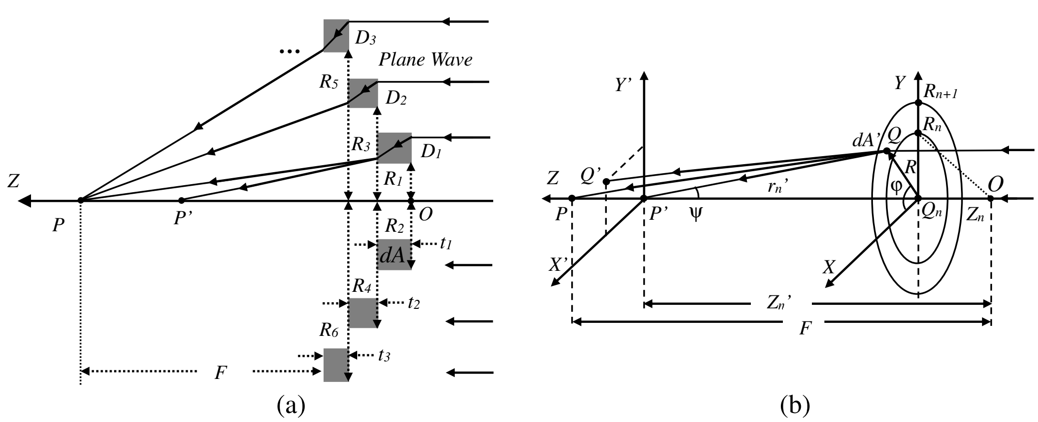

Figure 1. (a) Section geometry of the designed lens. (b) Focusing action of an annular flat ring.

According to Eq. (1), the focusing field $E_n(r'_n)$ produced at the point P' by the total annular ring can be expressed as

$$E_n(r'_n) = \frac{j}{\lambda} E_0(Z'_n) e^{-j\Delta\Phi_n} \int_0^{2\pi} \int_{R_n}^{R_{n+1}} H(\psi) \frac{e^{-j\beta r'_n}}{r'_n} R dR d\varphi \tag{2}$$

The focusing field $E_n(\rho'_n)$ produced at point $Q'(X',\, Y',\, Z')$ by the annular ring is

$$E_n(\rho'_n) = \frac{j}{\lambda} E_0(Z'_n) e^{-j\Delta\Phi_n} \int_0^{2\pi} \int_{R_n}^{R_{n+1}} H(\psi) \frac{e^{-j\beta\rho'_n}}{\rho'_n} R dR d\varphi \tag{3}$$

In Eq. (3), the Huygens source factor can be calculated by

$$H(\psi) = \frac{1+\cos\psi}{2} = \frac{\rho'_n + Z'_n - Z_n}{2\rho'_n} \tag{4}$$

The distance between the unit dA' and the point $Q'(X', Y', Z')$ is

$$\rho'_n(X', Y', Z', R, \varphi) = \sqrt{(X' - R\cos\varphi)^2 - (Y' - R\sin\varphi)^2 - (Z'_n - Z_n)^2} \tag{5}$$

The focusing field produced at point $Q'(X', Y', Z')$ by n annular rings can be expressed as

$$E(X', Y', Z') = \sum_n E_n(\rho'_n), \quad n = 1, 2, 3, \ldots, N \tag{6}$$

After the refraction of the lens, the intensity of the focusing field on the axis Z is defined as

$$I_F(Z') = \left[\frac{E(Z')}{E_0(Z')}\right]^2 \tag{7}$$

At the primary focal point P, where $Z' = F$, the focusing intensity (focusing gain, FG) in decibels can be expressed as

$$FG = I_F(F) = 20\log\left[\frac{E(F)}{E_0(F)}\right] \tag{8}$$

For the given design wavelength $\lambda = 857.1\,\mu\text{m}$ and focal length $F = 30\,\text{mm}$, the radius R_n and thickness w_n of the annular flat ring can be calculated by [17, 18]

$$R_n = \sqrt{2\Lambda(n)F + \Lambda^2(n)} \tag{9}$$

$$w_n = R_{n+1} - R_n \tag{10}$$

where $\Lambda(n) = n\lambda/2$ is a half-wave zone function and w_n the thickness of the n-th ring.

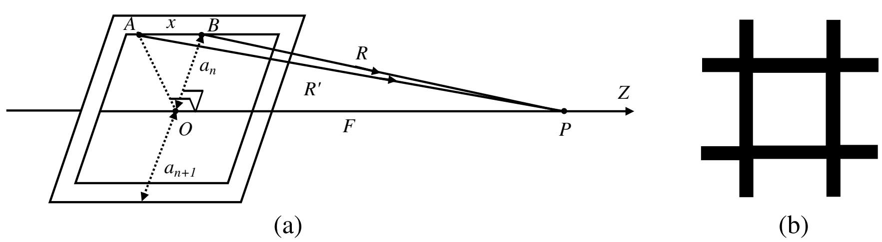

Figure 2. (a) Focusing action of a single square ring lens, (b) hatch-cross.

As mentioned above, most common FZP designs have circular shape zones. However, the polygonal Fresnel zones can be designed by substituting the circular shape of the Fresnel zones by a polygonal one. The simplest polygonal shape is triangle, although square, due to its nature fitting to the rectangular coordinate system, deserves special attention. The zones obtained using polygonal boundaries are an approximation to the actual Fresnel zones by using the paraxial approximation. As can be seen from Eq. (9) above, in the case of $F \gg n_{\max}\lambda$, the second term within the square root is negligible compared with the first term. Then Eq. (9) can be approximated by $r_n = (nF\lambda)^{1/2}$ which can be used to describe the apothem of the square Fresnel zone. Based on that, the square Fresnel zones (rings) shown in Figure 2(a) above have been built, whose apothems can be calculated by

$$a_n = \sqrt{nF\lambda} \tag{11}$$

As shown in Figure 2(a), there is a phase difference between the rays originating from the ring's center and the other rays in the course of reaching the focal plane which is unavoidable in polygonal Fresnel zones (rings). The optical path difference between the two rays originating respectively from point A and B is $\Delta = R' - R = x^2/2F$. Thus, when rays are launched from corners of the square ring, the phase difference will achieve the maximum and further impact the focusing action. Therefore, to reduce the adverse impact due to the corners and improve the focusing characteristics of the square ring, the hatch-cross (Figure 2(b)) is presented by extending the boundaries of the square ring to compensate the phase difference [19].

3. MODELING OF THZ LENS ANTENNA

The lens antenna consists of two parts: (1) the diagonal horn antenna; (2) the multilayer stacked lens. Design objectives of the lens antenna are axisymmetric radiation patterns with high gain and good directionality. All computer simulations in the article are completed by the CST 2015 software.

3.1. The Primary Feed Antenna

A diagonal horn antenna shown in Figure 3 is designed numerically firstly. The main structure parameters are: $W = 8.5\,\text{mm}$, $H = 7.3\,\text{mm}$, $w = 0.71\,\text{mm}$, $h = 0.355\,\text{mm}$, $L = 46\,\text{mm}$, $d = 4.6\,\text{mm}$. The width and height of the waveguide are determined to match the WR-2.8 rectangular waveguide (frequency ranging from 260 GHz to 400 GHz).

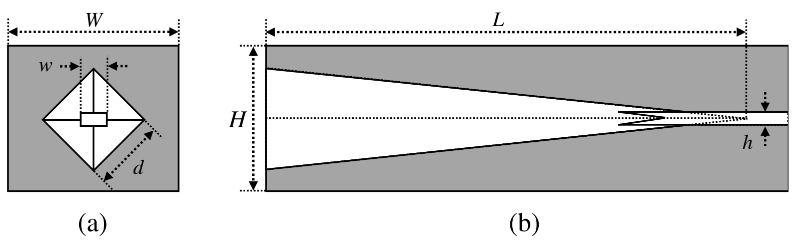

Figure 3. The sketch of the diagonal horn antenna. (a) Top view, (b) axial plane-cut view.

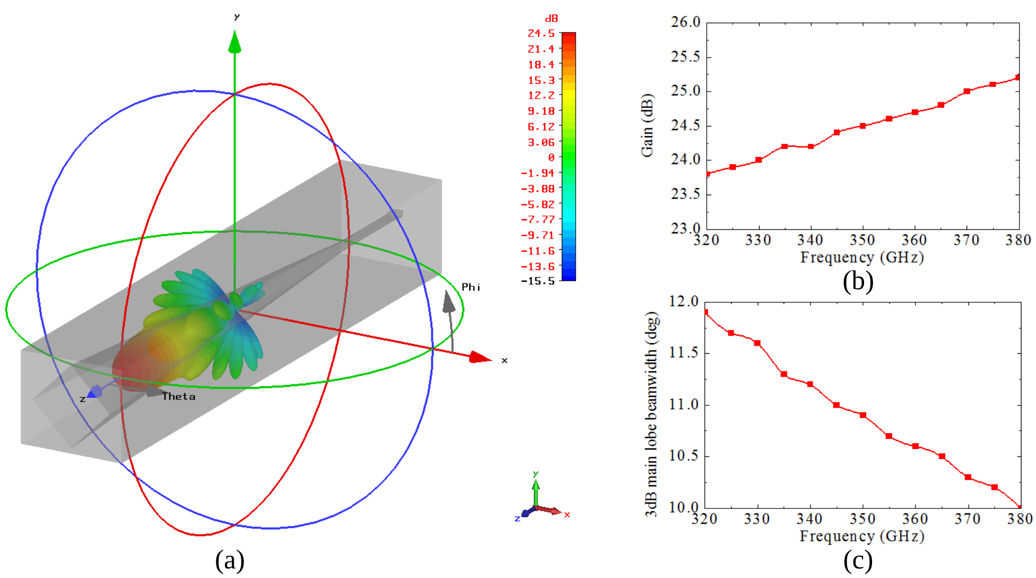

Figure 4. The far-field radiation characteristics of the diagonal horn antenna. (a) 3D antenna patterns at 350 GHz, (b) gain, (c) 3 dB main lobe beamwidth.

The far-field radiation characteristics of the diagonal horn antenna are shown in Figure 4.

1) 3D antenna patterns at 350 GHz: The antenna patterns under the condition that $-180° \leq \theta \leq 180°$ and $-180° \leq \varphi \leq 180°$ at 350 GHz are shown in Figure 4(a), where θ and φ are defined as the angles on the XZ plane and the XY plane, respectively, which are commonly used to make a more intuitive description in 3D space. It can be found that the diagonal horn antenna has axisymmetric radiation patterns with a tall and sharp main lobe.

2) Gain: The gain presented in Figure 4(b) is more than 23.8 dB across the band with a smooth upward trend. It is 24.5 dB at 350 GHz, and the maximum of 25.2 dB occurs at 380 GHz.

3) 3 dB main lobe beamwidth: Figure 4(c) reveals that the 3 dB main lobe beamwidth in the whole bandwidth shows a descending curve ranging from 11.9° to 10°. Therefore, half of the radiation power is confined in a small range, the diagonal horn has a good directionality.

Above results suggest that the diagonal horn antenna conforms to requirements of lens antennas due to the axisymmetric radiation patterns with high gain and good directionality.

3.2. Multilayer Stacked Lens Antenna

Based on the theoretical analysis and the lens geometry in Figure 2(b), the multilayer stacked lens is designed and studied. Figure 5 shows the 3D and top view of the lens prototype consisting of four concentric hatch-crosses which are stacked tightly one by one. All lens are made of fine copper for the center operation frequency $f = 350$ GHz. The lens is placed in front of the diagonal feed antenna at a distance of $D = F = 30$ mm. The lens is concentric with the center line of the diagonal horn antenna.

Based on Eqs. (10)–(11), the structure parameters of the lens are calculated and listed in Table 1. The thicknesses of Ring 1–4 are 2.10 mm, 1.36 mm, 1.08 mm and 0.82 mm, respectively.

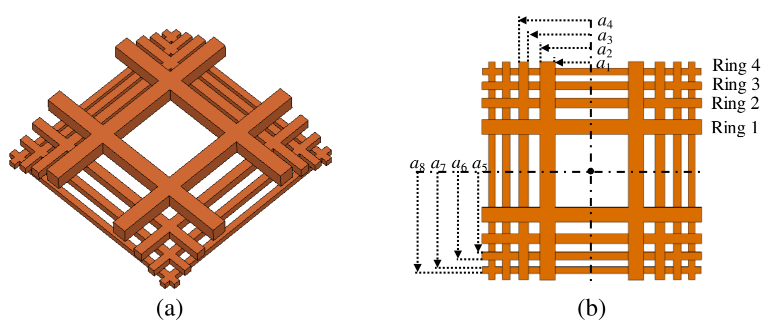

Figure 5. (a) 3D view of the lens, (b) top view and structure parameters of the lens.

Table 1. The structure parameters of the lens.

parameters	a_1/ mm	a_2/ mm	a_3/ mm	a_4/ mm	a_5/ mm	a_6/ mm	a_7/ mm	a_8/ mm
value	5.07	7.17	8.78	10.14	11.34	12.42	13.42	14.34

The far-field radiation characteristics of the lens antenna (4 layers) are shown in Figure 6.

1) 3D antenna patterns at 350 GHz: The antenna patterns under the condition that $-180° \leq \theta \leq 180°$ and $-180° \leq \varphi \leq 180°$ at 350 GHz presented in Figure 6(a) show that the designed lens antenna has axisymmetric radiation patterns with an obviously sharper main lobe compared with the diagonal horn antenna, which indicates that the lens antenna has an more focused power radiation. Further, the gains of the first side lobe and the second side lobe are 7.3 dB and 5.2 dB, respectively. Therefore, the first side lobe suppression ratio and the second side lobe suppression ratio are 20.4 dB and 22.5 dB, respectively.

2) Focusing gain: The focusing gain versus frequency graph shown in Figure 6(b) indicates that the focusing gain of the lens antenna is more than 27.1 dB in the whole frequency range and roughly 3.5 dB higher than the primary feed antenna. The maximum gain is 28.4 dB at 380 GHz.

3) 3 dB main lobe beamwidth: Figure 6(c) indicates the 3 dB main lobe beamwidth versus frequency curves of both the lens antenna (red line) and the horn antenna (green line). It is found that the 3 dB main lobe beamwidth of the lens antenna ranges from 4.3° to 5.4° throughout the entire working band. It has decreased by 61% at 350 GHz compared with the primary feed antenna. Hence, the radiation power is confined in a smaller range. The lens antenna has a great improvement in directionality.

The far-field characteristics shown in Figure 6 indicate that the lens antenna has axisymmetric radiation patterns. Compared with the primary diagonal horn feed antenna, the lens antenna has achieved a roughly 25% higher gain. In addition, power radiation is far more focused which implying a markedly improved directionality.

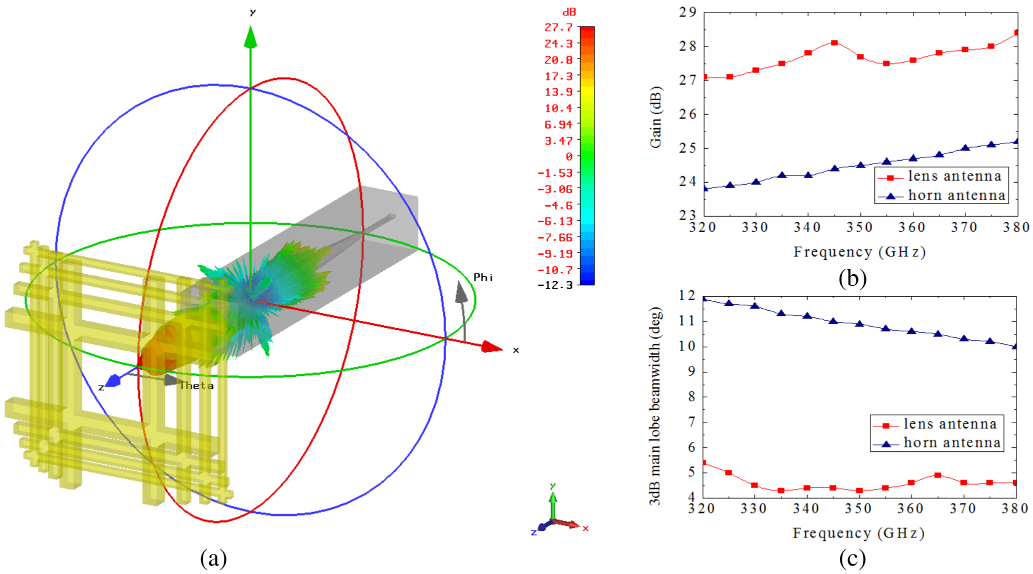

Figure 6. The far-field radiation characteristics of the lens antenna. (a) 3D antenna patterns at 350 GHz, (b) gain, (c) 3 dB main lobe beamwidth.

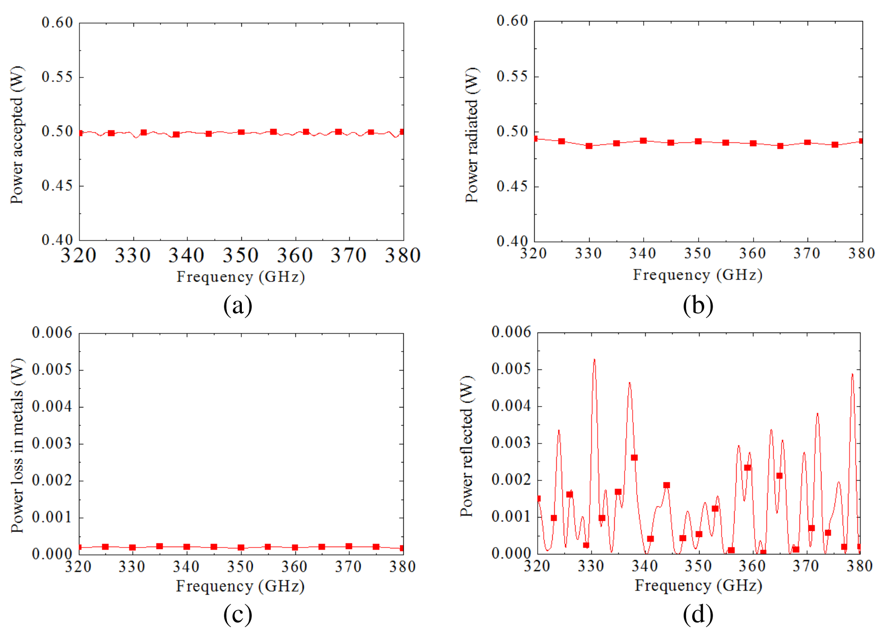

Figure 7. The power (RMS) of the lens antenna in Watt. (a) Accepted power, (b) radiated power, (c) power loss in metals, (d) reflected power.

Further, the losses are extremely important to describing the performance of the lens antenna since the power in THz is limited. The accepted power, radiated power, power loss in metals and reflected powers in RMS are shown in Figure 7. As can be calculated according to Figures 7(a) and (b), the value of the radiated power versus accepted power of the lens antenna is 98.3% at the center operation frequency of 350 GHz and higher than 97.8% across the whole frequency band which indicates that the lens antenna can radiate the most accepted power. Besides, both the reflected power and the power loss in metals are lower than 0.0053 W which is about 1.06% of the accepted power or the radiated power in the entire frequency band. To briefly conclude, the designed lens antenna is qualified for applications in THz wireless communication systems.

3.3. Structural Characteristics of the Lens Antenna

According to the configuration, the number of periods of lens p is the main structural property of the designed lens antenna. Additionally, the designed lens has the characteristic of multifocal according to the Fresnel-Kirchhoff diffraction theory. It means that the focus diameter ratio k ($k = F/D$) of the lens antenna also influences the lens antenna's far-field radiation patterns. To investigate the effects of the number of periods of the lens and the focus diameter ratio on radiation characteristics, variable-controlling approach has been used.

3.3.1. The Effect of the Number of Periods of the Lens on Radiation Characteristics

Firstly, the effect of the number of periods of the lens on antenna radiation properties is studied. Lens antennas with same focus diameter ration $k = 1$ (the lens is placed in front of the diagonal horn antenna at a distance of $D = F = 30$ mm), but different numbers of periods of the lens ($p = 3$, 4, 5, 6) are computed and compared.

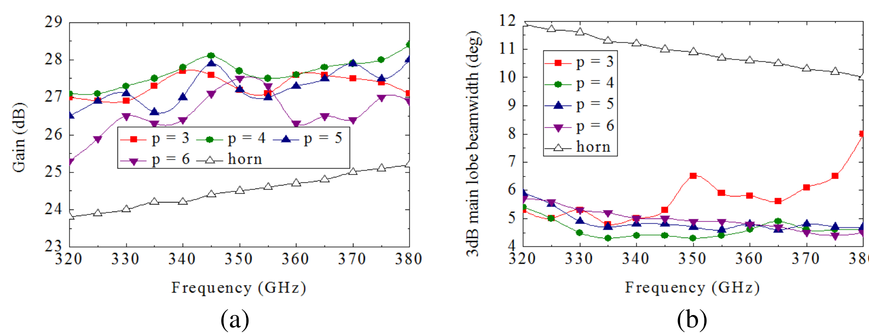

Figure 8. The far-field radiation characteristics of lens antennas with different numbers of periods of the lens and the primary feed antenna. (a) Gain, (b) 3 dB main lobe beamwidth.

As shown in Figure 8, the variation range of gain versus frequency curves of $p = 3$, 4, 5, 6 grows larger along with the increase of the number of periods of the lens. When $p = 4$, the gain varies from 27.1 to 28.4 dB, and the maximum gain is obtained at 380 GHz. Compared with the other lens antennas, the lens antenna on condition that $p = 4$ has a higher gain in the whole operation bandwidth. In addition, it is found that the lens antenna of $p = 4$ has a lower 3 dB main lobe beamwidth than other three lens antennas in the band ranging from 325 to 362 GHz, and it has the lowest average value of roughly 4.6°, which is 58% lower than the average value of the primary feed antenna. To briefly summarize, the optimal radiation properties of gain and directionality are obtained by the lens antenna on condition that $p = 4$ when the focus diameter ratio remains constant.

3.3.2. The Effect of the Focus Diameter Ratio on Radiation Characteristics

Based on the investigation in Subsubsection 3.3.1, the optimal performance of the lens antennas is obtained under the condition of $p = 4$ while the focus diameter ratio remains constant ($k = 1$).

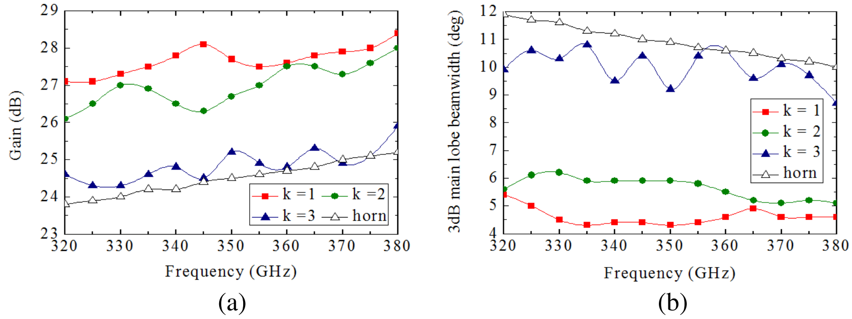

Figure 9. The far-field radiation characteristics of lens antennas with different focus diameter ratios and the primary feed antenna. (a) Gain, (b) 3 dB main lobe beamwidth.

Next, the effect of multifocal on antenna radiation properties will be studied. Lens antennas with the same number of periods of the lens $p = 4$, but different focus diameter ratios ($k = 1, 2, 3$) are computed and compared. As shown in Figure 9, compared with other lens antennas, the lens antenna of $k = 1$ has a higher gain and lower 3 dB main lobe beamwidth throughout the entire operation band. Therefore, the optimal radiation properties are achieved by the lens antenna with focus diameter ratio $k = 1$ when the number of periods of the lens is constant. In conclusion, the optimal antenna performance is obtained under the condition of $p = 4$, $k = 1$.

4. TEST PROCEDURE AND RESULTS

Experimental test for the lens antenna has been carried out. Since Teflon material has a high transmittance and low attenuation for terahertz waves [20], the four concentric hatch-crosses are assembled by using the Teflon double-sided tape. The thin tape is made of Teflon material, and the main ingredient of the glue on the tape is high temperature silica gel. The above tape has been used only on the contact points between the four hatch-crosses. The prototype of the lens made of fine copper is illustrated in Figure 10.

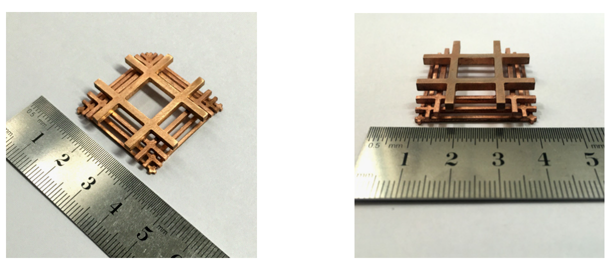

Figure 10. The prototype of the designed lens.

Figure 11 presents the sketch of the experimental set-up. The lens is illuminated by the transmitting diagonal horn antenna which is fed by a frequency multiplier from a distance of $D = 30$ mm. A receiver unit matching the transmitter can make stepping movements on the sliding rail. The transmitting antenna, lens and receiving antenna are center aligned in a horizontal line $H = 20$ cm away from the optical test platform. The distance between the lens and receiving antenna L can be calculated by [21].

$$L{=}2R^2/\lambda_{\min}{=}\ 4.7\,\mathrm{m} \tag{12}$$

where R is the maximum diameter size. To ensure all waves in the operation bandwidth satisfy the far-field condition, $\lambda_{\min}$ is the corresponding wavelength of the maximum frequency 380 GHz.

To get the far-field radiation patterns of the lens antenna, the receiver unit should move with a stepped angle of $\Delta\theta$ in a circle whose center is at the lens' caliber center during the test, as shown in Figure 11(c). However, circular movements of the receiver unit are difficult to operate practically as the

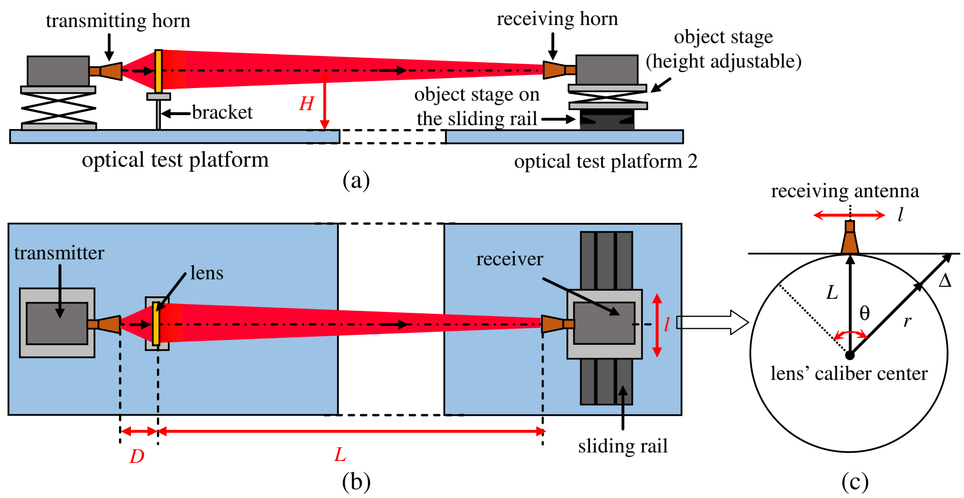

Figure 11. The (a) side view and (b) top view of the experimental set-up, (c) movements of the receiver unit during the test procedure.

value of L is quite large. Therefore, circular movements are replaced with linear movements on a sliding rail in a certain angle range. When $\theta = 7°$, $\Delta = r - L = L(1 - \cos\theta)/\cos\theta = 7.5 \times 10^{-3}L$ is negligible compared with L. The experimental scanning set up allows accurate measurements while θ ranges from $-7°$ to $7°$ (which contains main lobes of both the diagonal horn antenna and the lens antenna).

Based on the above experimental setup, the far-field characteristics of both the horn antenna and lens antenna have been tested and shown in Figure 12 and Figure 13, respectively. The tested gain of the horn antenna varies from 23.8 dB to 24.9 dB with the same variation tendency of the simulation graph. The tested 3 dB main lobe beamwidth is in agreement with the simulation results in general within the range of 10.8° to 12.4°. As for the proposed lens antenna, the tested gain graph has a slightly oscillation compared with the simulation. However, the focusing gain at 350 GHz is 27.1 dB, only 0.6 dB lower than the simulation results. Additionally, as can be seen from Figure 13(b), the tested 3 dB main lobe beamwidth of the proposed lens antenna ranges from 3.6° to 4.8°, lower than the simulation graph across the frequency band.

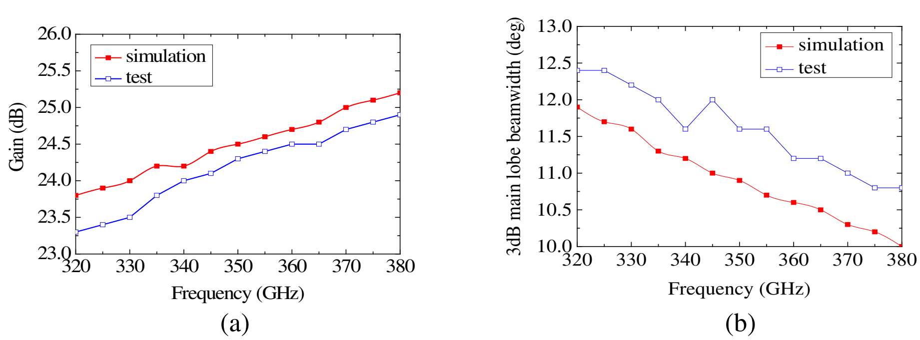

Figure 12. Measurement of the diagonal horn antenna. (a) Gain, (b) 3 dB main lobe beam width.

As can be seen from Figure 12 and Figure 13, there is disagreement between the simulation results and the tested ones. The main reasons are as follows:

1) Measurement method: In the practical experiment process, the circular movements of the receiver unit are replaced with linear movements on a sliding rail. The approximation leads to the facts that the test gain is lower than the simulation results owing to the extra distance Δ. Besides, in order to facilitate measurement, the step angle $\Delta\theta$ is 0.2° which may leads to a slightly inaccuracy in 3 dB main lobe beamwidth.

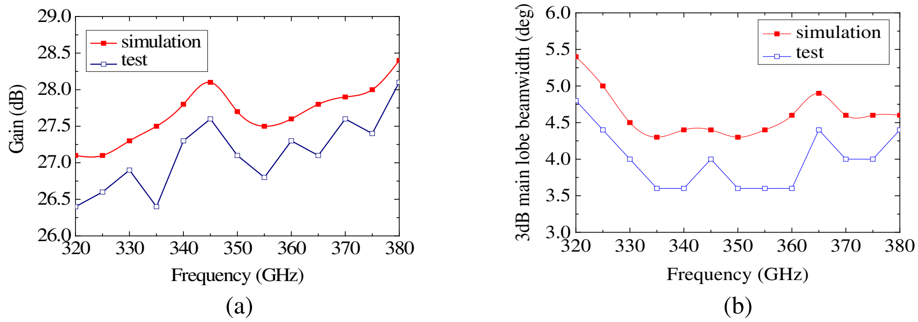

Figure 13. Measurement of the lens antenna. (a) Gain, (b) 3 dB main lobe beam width.

Besides, the receiving antenna was making lateral relative movements to the transmitting antenna on the sliding rail during the test, which leads to a consequence that the aperture of the receiving antenna has not been facing the lens. Therefore, the tested 3 dB main lobe beamwidth of the proposed lens antenna is lower than the simulation graph across the frequency band.

2) The manufacturing tolerances: There must be manufacturing tolerances during the process in which the diagonal horn antenna and the lens were fabricated or assembled which will lead to unavoidable and uncertain measurement errors.

5. CONCLUSIONS

In this article, a novel THz lens antenna is designed. A diagonal horn is adopted as the primary feed antenna, and a multilayer stacked lens is used to focus the electromagnetic waves. The Fresnel-Kirchhoff diffraction theory and paraxial approximation are used to analyze the focusing field of the designed lens. Effects of the number of periods of the lens and focus diameter ratio on antenna radiation characteristics are studied by using variable-controlling approach. Experimental test is carried out. The test results indicate that the designed lens antenna has a high gain over 26.4 dB and a low 3 dB main-lobe beamwidth less than 4.8° throughout the whole operation bandwidth. Due to the good focusing properties and directionality, the novel lens antenna is a qualified candidate for applications in THz wireless communication systems.

ACKNOWLEDGMENT

This work has been supported by the projects cstc2014zktjccxBX0065 and cstc2015zdcy-ztzx40003.

REFERENCES

1. Dufour, D., L. Marchese, M. Terroux, et al., "Review of terahertz technology development at INO," *Journal of Infrared, Millimeter, and Terahertz Waves*, Vol. 36, No. 10, 922–946, 2015.
2. Thampy, A. S. and S. K. Dhamodharan, "Performance analysis and comparison of MWCNT loaded ITO and TIO based optically transparent patch antennas for terahertz communications," *Physica E: Low-dimensional Systems and Nanostructures*, Vol. 78, 123–129, 2016.
3. Yang, Y., M. Mandehgar, and D. Grischkowsky, "THz-TDS characterization of the digital communication channels of the atmosphere and the enabled applications," *Journal of Infrared, Millimeter, and Terahertz Waves*, Vol. 36, No. 2, 97–129, 2015.
4. Melinger, J. S., Y. Yang, M. Mandehgar, et al., "THz detection of small molecule vapors in the atmospheric transmission windows," *Optics Express*, Vol. 20, No. 6, 6788–6807, 2012.
5. Hirata, A. and M. Yaita, "Ultrafast terahertz wireless communications technologies," *IEEE Transactions on Terahertz Science and Technology*, Vol. 5, No. 6, 1128–1132, 2015.

6. Lin, C. and G. Y. Li, "Adaptive beamforming with resource allocation for distance-aware multi-user indoor terahertz communications," *IEEE Transactions on Communications*, Vol. 63, No. 8, 2985–2995, 2015.
7. Ma, H. F., X. Chen, X. M. Yang, et al., "A broadband metamaterial cylindrical lens antenna," *Chinese Science Bulletin*, Vol. 55, No. 19, 2066–2070, 2010.
8. Jha, K. R. and G. Singh, "Ring resonator-integrated hemi-elliptical lens antenna," *Terahertz Planar Antennas for Next Generation Communication*, 83–105, Springer International Publishing, 2014.
9. Pascal, O., F. LemaÎtre, and G. Soum, "Design of a Gaussian optic lens antenna and effective parameters study," *Annales des Télécommunications*, Vol. 53, Nos. 3–4, 145–153, Springer-Verlag, 1998.
10. Karimkashi, S. and A. A. Kishk, "Focusing properties of Fresnel zone plate lens antennas in the near-field region," *IEEE Transactions on Antennas and Propagation*, Vol. 59, No. 5, 1481–1487, 2011.
11. Llombart, N., G. Chattopadhyay, A. Skalare, et al., "Novel terahertz antenna based on a silicon lens fed by a leaky wave enhanced waveguide," *IEEE Transactions on Antennas and Propagation*, Vol. 59, No. 6, 2160–2168, 2011.
12. Singh, N., C. K. Choure, M. Chauhan, et al., "Performance comparison of phase shifting surface lens antenna with other lens antennas," *2014 International Conference on Power, Control and Embedded Systems (ICPCES), IEEE*, 1–6, 2014.
13. Aragon-Zavala, A., *Antennas and Propagation for Wireless Communication Systems*, John Wiley & Sons, 2008.
14. Kamburov, L. P., J. M. Rodriguez, J. R. Urumov, et al., "Millimeter-wave conical fresnel zone lens of flat dielectric rings," *IEEE Transactions on Antennas and Propagation*, Vol. 62, No. 4, 2140–2148, 2014.
15. Ooi, B. L., Y. J. Fan, M. S. Leong, et al., "PSTD-FDTD analysis for complex irregular fresnel zone plates," *The Second European Conference on Antennas and Propagation, EuCAP 2007*, 1–6, 2007.
16. Hristov, H. D., L. P. Kamburov, J. R. Urumov, et al., "Conical double-dielectric fresnel zone lens and antenna," *Microwave and Wireless Components Letters, IEEE*, Vol. 17, No. 5, 325–327, 2007.
17. Minin, I. V. and O. V. Minin, *Diffractional Optics of Millimetre Waves*, CRC Press, 2004.
18. Liu, Y. and Y. Ge, "Design of high efficiency broadband fresnel zone lens antenna at K band," *2015 IEEE 4th Asia-Pacific Conference on Antennas and Propagation (APCAP)*, 317–318, 2015.
19. Sabatyan, A. and J. Rafighdoost, "Focusing specification of cross-like Fresnel zone plate," *Optik-International Journal for Light and Electron Optics*, Vol. 126, No. 24, 4796–4799, 2015.
20. Goto, M., A. Quema, H. Takahashi, et al., "Teflon photonic crystal fiber as terahertz waveguide," *Japanese Journal of Applied Physics*, Vol. 43, No. 2B, L317, 2004.
21. Stutzman, W. L. and G. A. Thiele, *Antenna Theory and Design*, John Wiley & Sons, 2012.